ELSEVIER

Journal of African Earth Sciences 36 (2003) 89–98

Journal of African Earth Sciences

www.elsevier.com/locate/jafrearsci

Global Neoproterozoic (Sturtian) post-glacial sulfide-sulfur isotope anomaly recognised in Namibia

Paul Gorjan [a], Malcolm R. Walter [a,*], Roger Swart [b]

[a] *Australian Centre for Astrobiology, Macquarie University, North Ryde, Sydney, NSW 2109, Australia*
[b] *NAMCOR (National Petroleum Corporation of Namibia), Private Bag 13196, Windhoek, Namibia*

Received 14 March 2002; accepted 4 December 2002

Abstract

The Neoproterozoic Earth experienced at least two, probably global, glaciations. Each glaciation was superceded by deposition of a layer of carbonate ('cap-carbonate') that has a distinctive lithology and depletion in ^{13}C ($\delta^{13}C_{carbonate} \sim -5‰$). The ~700 Ma Sturtian glaciation is followed by deposition of a cap-carbonate and post-glacial succession which contain bacterially produced sulfides extremely enriched in ^{34}S (average $\delta^{34}S_{sulfide} \sim +30‰$) with maximum values up to +60‰. This level of ^{34}S enrichment in sulfides is unique to the Sturtian post-glacial succession and recognised in Australia, Canada, and China. In the Neoproterozoic of the Nama Basin, Namibia, the Gobabis Member is the basal unit of the Court Formation, which overlies the glacial Blaubeker Formation. $\delta^{13}C_{carbonate}$ analyses from the Gobabis Member range from −5.2 to −2.2‰ (average = −3.7‰; n = 10). $\delta^{34}S_{sulfide}$ ranges from +16.1 to +61.1‰ (average = +37.6‰; n = 8). These results are consistent with a Sturtian age for the Blaubeker Formation and overlying Gobabis Member, which have previously been interpreted as Sturtian. The sulfur isotopic results are comparable with $\delta^{34}S_{sulfide}$ in Sturtian post-glacial units of Australia, Canada and China. This adds to the evidence for correlation of the Blaubeker Formation with Sturtian glaciations on other continents. The cause of such elevated $\delta^{34}S_{sulfide}$ is enigmatic. Geochemical evidence suggests the sulfide was not formed from low sulfate waters nor in euxinic conditions, which discounts any known modern analogue. ^{34}S enrichment in sulfides is therefore postulated to be caused by enrichment of ^{34}S in contemporaneous seawater ($\delta^{34}S_{sulfate}$ up to +60‰?). The rise in seawater $\delta^{34}S_{sulfate}$ is considered to be the result of intense bacterial sulfate reduction in an anoxic ocean during the Sturtian glaciation.

Keywords: Neoproterozoic; Sulfur-isotopes; Sturtian glaciation; Sturtian post-glacial; Snowball Earth

1. Introduction

The Neoproterozoic is characterised by at least two, probably global, glacial events. The oldest documented of these is Sturtian (~700 Ma; Walter et al., 2000). Neoproterozoic glacial units are frequently overlain by laminated carbonates, forming 'caps' to the glacial units (Kennedy et al., 1998). The Sturtian cap carbonates are generally dark, organic-rich dolomite; whereas the younger Marinoan glacial cap is pale (cream, pink, or tan) and organic-poor (Kennedy, 1996; Hoffman et al., 1998a; Kennedy et al., 1998). $\delta^{13}C_{carbonate}$ values of Sturtian cap carbonates are ~−5‰ in Australia and up to −6‰ in Canada (Kaufman et al., 1997; Walter et al., 2000). Sturtian cap carbonates are typically overlain by siltstone. In Australia (Tapley Hill and Aralka Formations), China (Datangpo Formation) and Canada (Twitya Formation) these Sturtian post-glacial successions have extremely ^{34}S-enriched sulfides, with a mean $\delta^{34}S_{sulfide}$ of +30‰ (Gorjan et al., 2000).

In the Nama Basin (Fig. 1) the oldest Neoproterozoic glacial horizon is the Blaubeker Formation, it is therefore interpreted to be the Sturtian glacial (Hegenberger, 1993). The Blaubeker Formation underlies the post-glacial Court Formation, of the Witvlei Group, which has the carbonate-rich Gobabis Member at its base. Previous $\delta^{13}C_{carbonate}$ analyses from the Gobabis Member range from −3 to +2‰ (n = 3) (Kaufman et al., 1991). Here we present new $\delta^{34}S_{pyrite}$ and $\delta^{13}C_{carbonate}$ data from the Gobabis Member intercepted in Tahiti-1 drillhole (22°57′09″S, 18°43′28″E: northern Nama Basin,

* Corresponding author. Tel.: +61-2-4457-1565; fax: +61-2-4457-1566.
E-mail address: malcolm.walter@mq.edu.au (M.R. Walter).

0899-5362/03/$ - see front matter © 2003 Elsevier Science Ltd. All rights reserved.
doi:10.1016/S0899-5362(03)00002-2

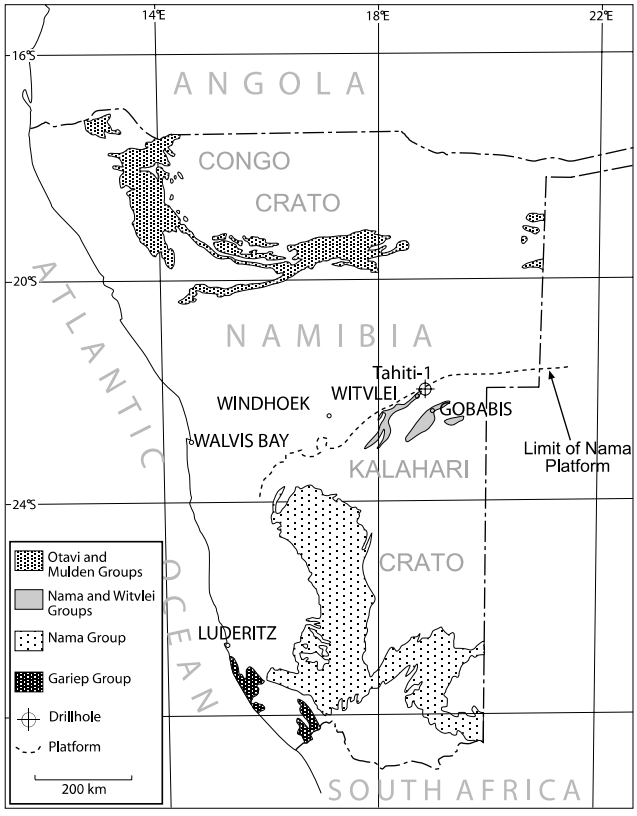

Fig. 1. Map showing Namibian Neoproterozoic outcrop (after Kaufman et al., 1991) and location of drillhole Tahiti-1.

east of Windhoek) that are consistent with a Sturtian age for the Blaubeker Formation. We also interpret the data in terms of global correlations and discuss the origin of such ^{34}S-enriched sulfides.

2. Methods

In sedimentary rocks sulfur can exist as pyrite (FeS_2), iron monosulfide (FeS as mackinawite, pyrrhotite or an amorphous phase), elemental sulfur (S^0), sulfate (SO_4^{2-}), or organically-bound sulfur. In this study iron monosulfide and pyrite were extracted from 1 to 5 g of crushed sample. Only the $\delta^{34}S$ of pyrite was analysed because it was overwhelmingly the most abundant form. The sulfur extraction procedure is based on the method presented in Canfield et al. (1986).

Firstly, monosulfide compounds (acid-volatile-sulfur, AVS) were removed from the crushed sample by reaction with 6 M hydrochloric acid (HCl) and tin(II) chloride ($SnCl_2$). The crushed sample was boiled for 5 min with reagents under flow of N_2. This converts AVS to hydrogen sulfide (H_2S) gas which is reacted with silver nitrate ($AgNO_3$) to form the extremely insoluble silver sulfide (Ag_2S).

Pyrite was then removed from the previously treated sample by reaction with ~1 M chromium(II) chloride ($CrCl_2$) solution that was added to the HCl, $SnCl_2$, and sample mixture. The mixture was then boiled until all H_2S was evolved from reaction of Cr^{2+} with pyrite. A flow of N_2 carried the H_2S through the apparatus and it was trapped as Ag_2S as the monosulfide extraction above. Ag_2S was collected by filtration, dried, and then weighed. The Ag_2S was stored in plastic sample tubes until conversion to SO_2 by reaction with copper(I) oxide (Cu_2O) at 1050 °C.

$\delta^{13}C_{carbonate}$ analysis used the standard method of phosphorolysis (McCrea, 1950). Isotopic determinations were carried out on a MAT-Finnigan 252 mass spectrometer. $\delta^{34}S$ results are presented against the CDT standard. $\delta^{13}C$ and $\delta^{18}O$ results are presented against the PDB standard. Errors for replicate samples are mostly within $\pm 0.5‰$ for sulfides and within $\pm 0.2‰$ for carbonates.

3. Stratigraphy and lithology

The Witvlei Group outcrops in central Namibia (Fig. 1), on the northern margin of the Kalahari Craton. It lies above the Tsumis and Nosib Groups and below the Nama Group in the northern Nama Basin. At the base of the Witvlei Group is the Court Formation which unconformably overlies diamictite of the Blaubeker Formation (Fig. 2). The Blaubeker Formation is interpreted as glacial because it is a widespread diamictite with faceted and striated heterolithic boulders (Hoffmann, 1989; Hegenberger, 1993). In Tahiti-1 the matrix of the diamictite contains abundant fine-grained carbonate, much of it as well-formed rhombs.

The Court Formation consists (from oldest to youngest) of the Tahiti Member (sandstone), Gobabis Member (dark carbonate), Constance Member (shale, siltstone), and Simmenau Member (sandstone, conglomerate) (see Fig. 2). In most Witvlei outcrop the Tahiti Member is absent, so the Gobabis Member forms the basal unit. The Gobabis Member consists of three facies. The basal facies is a finely laminated dark grey to black silty carbonate. Overlying this is a dark well-bedded to massive carbonate with intraclastic and (?)stromatolitic carbonate, and sandy carbonate. The third, 'beach', facies is sandy carbonate to calcareous sandstone but has only limited distribution (Hegenberger, 1993).

We sampled the Gobabis Member in drillhole Tahiti-1 where it is represented almost entirely by the finely laminated, basal facies. In outcrop near Tahiti-1 the Gobabis Member is also a thin-bedded, flat-laminated dark grey to black carbonate. The Gobabis Member in Tahiti-1 is 37.5 m thick, the top of the member being eroded. In Tahiti-1 it is dark grey to black silty shale

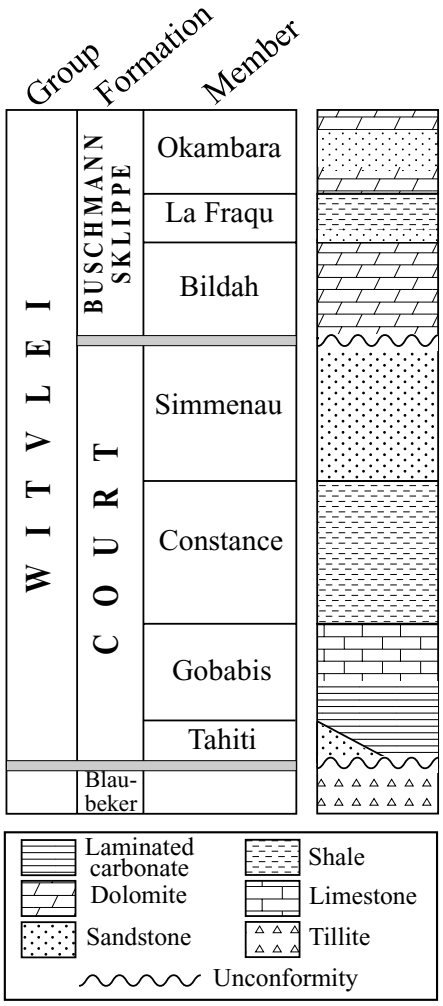

Fig. 2. Stratigraphy and idealised geological section of the Witvlei Group, Nama Basin, Namibia (after Hegenberger, 1993).

with abundant kerogenous and pyritic laminae, and kerogenous silty dolomite. The dolomite is anhedral with a grain size of 5–25 μm. Dolomite laminae are 50–1000 μm thick, separated by wispy silty and kerogenous lamine 10–100 μm thick. Pyrite occurs as grains and framboids 5–40 μm wide. There are small nodules and veins (parallel to cleavage) of a later generation of carbonate. There are some millimetre-scale lenses of fine-grained quartz sandstone, and one example of a carbonate-cemented carbonate sand with intraclasts of acicular carbonate crusts.

4. Results

Eight analyses of $\delta^{34}S_{pyrite}$ are shown in Fig. 3 and Table 1. It ranges from +16.1‰ to +61.1‰ (average = +37.6‰). The pyrite of the Gobabis Member is mostly framboidal and 5–40 μm diameter. Ten analyses of $\delta^{13}C_{carbonate}$ are shown in Fig. 2 and Table 2. Values range from −5.2‰ to −2.2‰ (average = −3.7‰). $\delta^{18}O_{carbonate}$ values ranged from −9.3 to −5.2‰ (average = −7.5‰). Fig. 2 shows no apparent trend in $\delta^{13}C_{carbonate}$, while $\delta^{34}S_{pyrite}$ apparently increases with decreasing age, although the trend is weak.

5. Discussion

5.1. Controls on seawater $\delta^{34}S_{sulfate}$

The $\delta^{34}S_{sulfate}$ of seawater is determined by the magnitude and $\delta^{34}S$ of fluxes in and out of the ocean. In the modern environment the major sulfur flux into the ocean comes from the weathering of the continents into riverine sulfate ($\delta^{34}S_{sulfate} \sim +7‰$). A lesser amount comes from hydrothermal sources ($\delta^{34}S_{sulfate} \sim +3‰$) (Charleson et al., 1992; Alt, 1995). The major fluxes of sulfur out of the ocean are the deposition of sulfate evaporites and sedimentary sulfides. Sulfate evaporites are deposited with minimal fractionation. But sulfide deposition, mediated by sulfate-reducing bacteria, involves a large fractionation. Laboratory experiments with sulfate-reducing bacteria report fractionation of upto 46‰ from the starting sulfate values, but fractionations upto 70‰ are noted in the natural environment (Nielsen, 1978). This bacterially mediated fractionation is the main reason for the positive $\delta^{34}S_{sulfate}$ value of seawater.

5.2. Fractionation of sulfur isotopes

Sulfate-reducing bacteria reduce sulfate to hydrogen sulfide (Goldhaber and Kaplan, 1974). The bacterially formed hydrogen sulfide reacts with sedimentary iron to form iron sulfides. Pyrite is the most stable iron-sulfide under normal conditions and therefore the most abundant form (Berner et al., 1979). Organic matter is the fuel for sulfate-reducing bacteria, which oxidise it to carbon dioxide, with concomitant reduction of sulfate to hydrogen sulfide (sulfate being the ultimate electron acceptor, as oxygen is in animal respiration).

Bacterial reduction of sulfate fractionates sulfur isotopes because the ^{32}S isotope is preferentially metabolised by the bacteria. This results in the sulfide being enriched in ^{32}S compared to the starting sulfate. In the Phanerozoic, sedimentary sulfides are typically enriched in ^{32}S between 0‰ and 70‰, with the bulk around 50‰, compared to the seawater sulfate (Nriagu et al., 1991; see also Fig. 2 in Canfield, 1998). Phanerozoic seawater $\delta^{34}S_{sulfate}$ values vary between ~+12 (at Permian–Triassic boundary) and ~+33‰ (at Proterozoic–Cambrian boundary) (Claypool et al., 1980; Holser, 1992). This means that sedimentary sulfides typically have a $\delta^{34}S$ value less than 0‰.

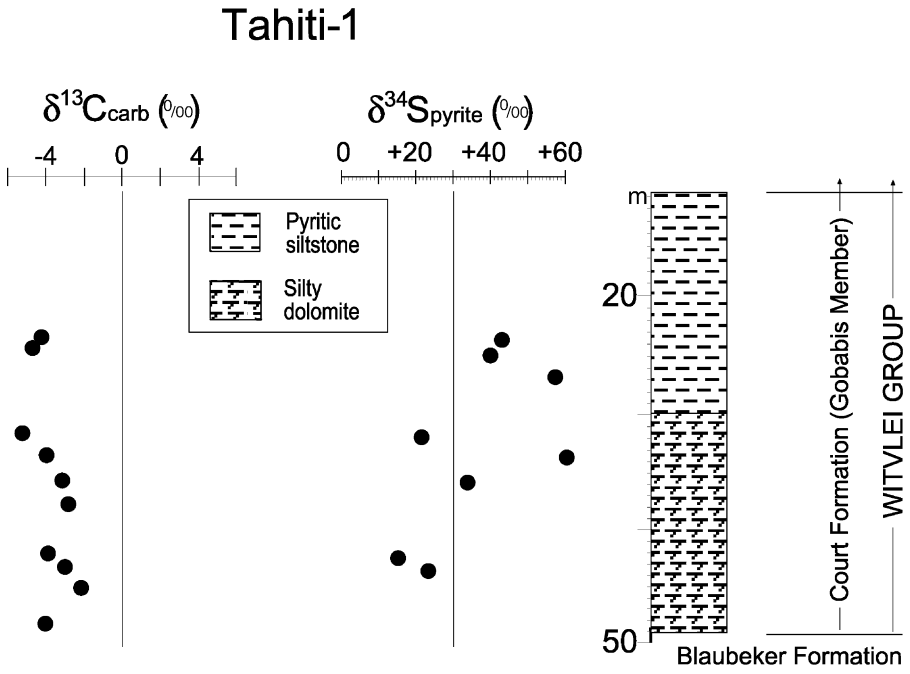

Fig. 3. $\delta^{13}C_{carbonate}$ and $\delta^{34}S_{pyrite}$ from the Tahiti-1 drillhole, Nama Basin, Namibia.

Table 1
$\delta^{34}S_{pyrite}$ analyses for the Gobabis Member in the Tahiti-1 drillhole

Depth (m)	$\delta^{34}S_{pyrite}$ (‰)
23.78	+43.3
24.80	+41.1
26.75	+58.1
31.95	+22.4
33.60	+61.1
35.70	+34.4
42.40	+16.1
43.59	+24.5

Table 2
$\delta^{13}C_{carbonate}$ and $\delta^{18}O_{carbonate}$ analyses for the Gobabis Member in the Tahiti-1 drillhole

Depth (m)	$\delta^{13}C_{carbonate}$ (‰)	$\delta^{18}O_{carbonate}$ (‰)
23.78	−4.2	−9.3
24.80	−4.6	−8.9
31.95	−5.2	−6.9
33.60	−4.0	−6.9
35.70	−3.3	−8.3
37.70	−2.9	–
42.40	−3.9	−5.2
43.59	−2.9	−7.1
44.36	−2.2	–
48.60	−4.0	–

Neoproterozoic seawater $\delta^{34}S_{sulfate}$ values appear to be similar to those of the Phanerozoic, but the variation is not as well constrained (Strauss, 1993; Strauss et al., 2001). Likewise, the seawater $\delta^{34}S_{sulfate}$ for Sturtian post-glacial time has so far eluded certainty. Sulfate minerals from the Tapley Hill Formation of Australia have a mean value of +26‰ (n = 5) (Gorjan et al., 2000), but may be altered. Hurtgen et al. (2002) report large swings in $\delta^{34}S_{sulfate}$ between 12‰ and 51‰, based on trace sulfate analysis. And methods to predict the $\delta^{34}S_{sulfate}$ from $\delta^{34}S_{pyrite}$ for this time give a possible range of +30 to +60‰. These methods include assuming $\delta^{34}S_{sulfate}$ equals the average $\delta^{34}S_{pyrite}$, as would occur where sulfate was limited, giving a value of +30‰ for Sturtian post-glacial time. Ross et al. (1995) suggest that $\delta^{34}S_{sulfate}$ equals the highest $\delta^{34}S_{pyrite}$. Which, in this case, would give a value of +60‰. However, both of these assumptions are unreliable (Gorjan et al., 2000).

Unlike Phanerozoic sedimentary sulfides, Sturtian post-glacial sedimentary sulfides are unusually enriched in ^{34}S (Fig. 3). In Canada and Australia the mean $\delta^{34}S_{pyrite}$ is ~+30‰. This is higher than seawater sulfate values for all geological time except near the Proterozoic–Cambrian boundary (where $\delta^{34}S_{sulfate}$ is +33‰; Claypool et al., 1980; Holser, 1992; Strauss, 1993; Shields et al., 2000). Such consistently high $\delta^{34}S_{sulfide}$ values for bacterially produced sulfide is unique in the geologic record.

The framboidal pyrite (5–40 μm) in the Gobabis Member is typical of sedimentary sulfides with a bacterial origin. It is also similar to that in Australian Sturtian post-glacial sediments, where framboidal pyrite is 1–60 μm (Gorjan, 1998, p. 147).

5.3. Global correlation

In the following any discussion of Namibian sediments is from Hegenberger (1993). The Blaubeker For-

mation consists of unsorted boulders and pebbles in an unstratified fine-sandy to shaly matrix. Boulders are faceted and striated indicating a glacial origin. The Gobabis Member is a dark carbonate, consisting of two main facies, a third has only minor distribution. The older is a laminite of alternating light and dark carbonate with sub-millimeter laminae. Organic content is 0.1–0.2%. The younger facies is a well-bedded to massive carbonate. The change in facies reflects a movement from deep to shallow-water environment. The older facies is very similar to that of Sturtian post-glacial successions in Australia (Tapley Hill and Aralka Formations) and Canada (Twitya Formation). The Marinoan cap carbonates are distinctly different. The Marinoan Bildah Member of the Witvlei Group is a thickly bedded to massive light-gray to pink dolomite, similar to Marinoan cap carbonates in other parts of Namibia (e.g., Maieberg Formation of the Otavi Group in northern Namibia; Hoffman et al., 1998a) and on other continents (Kennedy, 1996; Kennedy et al., 1998).

The $\delta^{13}C_{carbonate}$ values for the Gobabis member resemble those for correlative units in Namibia. The Sturtian post-glacial Wallekraal Formation (above the glacial Kaigas Formation) of the Hilda Subgroup of the Port Nolloth Zone, Namibia, has $\delta^{13}C_{carbonate}$ values of around $-4‰$ (Frimmel and Jiang, 2001). Yoshioka et al. (1999) also report a $\delta^{13}C_{carbonate}$ value of $-4.7‰$ at the base of the Sturtian post-glacial Rasthoff Formation (overlying Chuos diamictite, Otavi Group, northern Namibia). Halverson et al. (1999) report $\delta^{13}C_{carbonate}$ values around $-2‰$ in the same formation. Marinoan cap carbonates have similar $\delta^{13}C_{carbonate}$ values to Sturtian cap carbonates (Walter et al., 2000). Because of this $\delta^{13}C_{carbonate}$ cannot test between these caps. However, the extremely high $\delta^{34}S_{pyrite}$ values for the Sturtian post-glacial horizon are unique in their level of ^{34}S enrichment in pyrite. Marinoan cap carbonates have neither the same elevated average $\delta^{34}S_{pyrite}$ value ($\sim+30‰$ in the Sturtian) nor the same maximum values (up to $+60‰$ in the Sturtian) (see Fig. 12 in Gorjan et al., 2000). This allows the possibility of correlation between formations based on $\delta^{34}S_{pyrite}$. Correlation of the Blaubeker Tillite and Court Formation with Sturtian glacial and post-glacial successions on other continents (as shown in Fig. 3), suggested by the lithological similarities, is strengthened by the $\delta^{34}S_{pyrite}$ results from the Gobabis Member.

5.4. The origin of ^{34}S-enriched sedimentary sulfide

The correlation of the Gobabis Member with other Sturtian post-glacial successions raises the question of what conditions produced the enrichment of ^{34}S in sulfides on at least four continents. Situations in the modern environment known to produce ^{34}S-enriched pyrite are either low in sulfate (e.g., North American Great Lakes, Nriagu and Coker, 1976) or euxinic (e.g., Arctic Lakes, Jeffries and Krouse, 1985; Antarctic Lakes, Burton and Barker, 1980). Bacterial reduction of sulfate where there is a low sulfate concentration causes most or all of the sulfate to be reduced to sulfide so that the sulfur-isotopic composition of the sulfide approaches that of the starting sulfate. Bacterial reduction of sulfate in a euxinic environment can produce H_2S with greater $\delta^{34}S$ than the starting sulfate (although not explained in the above references it is presumably by diffusion of ^{32}S-enriched H_2S to upper layers of the water column). Ancient environments with ^{34}S-enriched sulfides are therefore interpreted to be the result of either low-sulfate concentrations or euxinic conditions (e.g., Devonian of the Selwyn Basin, Goodfellow and Jonasson, 1984; Green River Formation, Tuttle and Goldhaber, 1993).

Previous hypotheses to explain the elevated $\delta^{34}S_{pyrite}$ have also relied upon either low-sulfate concentrations or euxinic conditions. A Proterozoic ocean with low sulfate concentration and high $\delta^{34}S_{sulfate}$ has been proposed (Bottomley et al., 1992; Hayes et al., 1992). Lambert and Donnelly (1988) have suggested that the enrichment in ^{34}S is the result of sulfate limitation in intracratonic basins at least partially isolated from the global ocean. Logan et al. (1995) postulate the existence of a sulfate-minimum zone, analogous to the O_2-minimum zone in the modern oceans, where sulfate is depleted due to intense bacterial sulfate reduction leaving the residual sulfate with a higher than normal $\delta^{34}S$. However, geochemical evidence from the Sturtian post-glacial Tapley Hill and Aralka Formations (of Australia) suggests that the conditions could not have been low in sulfate nor euxinic. The evidence is as follows:

(i) %C and %S data from the Tapley Hill and Aralka Formations bulk samples analysed in Gorjan et al. (2000) show a positive correlation with an S/C ratio of 2:1 (Fig. 17 in Gorjan et al., 2000). This is consistent with an environment where sulfate reduction was limited by organic matter, not sulfate. Under low-sulfate conditions sulfate is the limiting factor and under euxinic conditions the supply of iron is the limiting factor in sulfide formation. When iron or sulfate is the limiting factor in sulfide formation there is no correlation between %C and %S of a sediment (Berner, 1984). The S/C ratio of 2:1 is typical of Neoproterozoic sediments containing sulfides of a bacterial origin (Strauss, 2002).

(ii) In Tapley Hill and Aralka Formation samples the $\delta^{34}S_{organic} > \delta^{34}S_{pyrite}$ (Gorjan, 1998, p. 144) which is consistent with a non-euxinic environment. This is because organic matter reacts with sulfide less readily than iron. Thus, organic matter will tend to react with the later-formed sulfide while the iron reacts with the earlier-formed sulfide in the sediment. The Rayleigh distillation process predicts that later-formed sulfide will be enriched in ^{34}S, compared to the earlier formed sulfide

(Thode, 1991). An euxinic environment would have $\delta^{34}S_{organic}$ equal to $\delta^{34}S_{pyrite}$ because of the supply of H_2S with a constant $\delta^{34}S$ (Tuttle and Goldhaber, 1993).

(iii) Molar FeS:FeS_2 ratios $\ll 1$ (Gorjan, 1998, p. 144) in Aralka and Tapley-Hill Formation samples also suggest sulfate-rich conditions. The amount of pyrite in Sturitan post-glacial successions far exceeds monosulfide compounds. Low-sulfate (freshwater) waters produce approximately equal amounts of FeS and FeS_2 (Berner et al., 1979).

(iv) Degree of pyritisation (DOP = Fe in pyrite/total Fe) indicates the degree to which iron in the sediment is converted to pyrite and high values (>0.8) are an indicator of euxinic conditions. Tapley Hill and Aralka Formation values are generally less than 0.5 (Fig. 18 in Gorjan et al., 2000) which is typical of non-euxinic conditions. Euxinic conditions produce high DOP values because there is much more sulfide available to react with iron (Raiswell et al., 1988).

(v) High sulfide contents (up to 2 wt.%) in Tapley Hill and Aralka Formation samples also suggest ample sulfate in overlying waters (Lambert and Donnelly, 1990).

Normal sulfate and non-euxinic conditions are also expected during deposition of correlative sediments that have ^{34}S-enriched pyrite in China (Datangpo and Minle Formations; Xu et al., 1990; Li et al., 1999), Canada (Twitya Formation; Hayes et al., 1992) and Namibia (Gobabis Member; this study). If we rule out euxinic and low-sulfate conditions as causing the ^{34}S-enriched sulfides, then the only other known cause is that they were derived from extremely ^{34}S-enriched sulfate, with a $\delta^{34}S$ perhaps up to +60‰ (Hayes et al., 1992; Gorjan et al., 2000). Gorjan et al. (2000) hypothesise that, at the conclusion of the Sturtian glacial period, there was a rapid rise in $\delta^{34}S_{sulfate}$. The ^{34}S-enrichment in seawater sulfate was the result of intense bacterial reduction of sulfate in an anoxic (possibly ice-covered) ocean during the Sturtian glaciation. Reduction occurring in the water column would have maximum fractionation because of the open-system conditions, and the product ^{32}S-enriched sulfide would be deposited on the ocean floor by reaction with iron that is supplied by increased hydrothermal discharge into the oceans (Walter et al., 2000). The residual sulfate would be enriched in ^{34}S. Also, glacial conditions would prevent the input of riverine sulfate ($\delta^{34}S_{sulfate} = +7‰$ in the modern environment; Nriagu et al., 1991) to the oceans, further increasing the oceanic $\delta^{34}S_{sulfate}$. Upon thawing sea level rose and the ^{34}S-enriched seawater flooded the continental shelves.

5.5. The origin of ^{13}C-depleted cap carbonates

The Neoproterozoic phenomenon of cap carbonates immediately overlying a glacial horizon has been recognised as paradoxical because it suggests a frozen environment is immediately followed by a tropical environment virtually everywhere (Hoffman and Schrag, 2002). Explanations must also take into account the depletion of ^{13}C in these carbonates. There are several competing hypotheses. Grotzinger and Knoll (1995) and Kaufman et al. (1997) have suggested that organic matter formed in the ocean's upper layers during the glacial period sank to anaerobic depths where it metabolised by bacterial sulfate reduction, thus producing ^{13}C-depleted dissolved inorganic carbon (DIC). At the end of glaciation the deep water upwelled depositing the DIC as cap carbonates. Hoffman et al. (1998b) and Hoffman and Schrag (2002) have suggested that organic matter production was insignificant in the glacial ocean, and DIC from hydrothermal input dominated, which has a $\delta^{13}C$ of $\sim -6‰$. Also, during the post-glacial period there was an intense weathering of the frost-shattered rock that would drive a flux of alkalinity depositing the carbonates. Kennedy et al. (2001) have suggested the carbonate caps are formed by seeping methane hydrate (formed in the glacial period and stored in the permafrost) in the post-glacial environment. Our results are most easily explained by the first hypothesis, where organic matter is the source of ^{13}C-depleted DIC.

5.6. Problems of the ocean-upwelling sulfur model

1. A Snowball Earth with the oceans frozen over does not readily allow for organic matter to be formed. It is recognised that cyanobacteria and eukaryotes survived a snowball Earth. McKay (2000) suggests that photosynthesis is possible beneath ice sheets upto 10 m thick, although productivity would be greatly reduced. This means that there would be a limited supply of organic matter to fuel sulfate-reduction. Hyde et al. (2000) have modelled a 'mild' Snowball Earth where ice-coverage does not extend to the oceans near the equator. This scenario would allow greater primary production in the equatorial ocean. Sedimentological work by Condon et al. (2002) on the Sturitan glacials shows that glacial rain-out continued during the glaciation suggesting that ice-sheets were mobile and the hydrologic cycle was functioning. This is further evidence for an unfrozen ocean.

Another limit to organic matter formation would be nutrient supply. In a stagnant ocean the upwelling of nutrients, as in a circulating ocean, would be inhibited (Hotinski et al., 2001). However, precise nutrient quantities and movements have not been established (see the Permian example in Hotinski et al., 2001). Also, it is possible that rock flour from glacial activity would supply some nutrients. Primary productivity based on hydrothermal energy is also possible, although this is unlikely to be a major contributor.

2. Although the ocean-upwelling model explains the sudden rise of $\delta^{34}S_{sulfide}$ it has difficulty in explaining the sudden decline at the close of post-glacial silt deposition (Tapley Hill Formation and global equivalents; see Fig. 4). If there was a single upwelling of ^{34}S-enriched sulfate (as the cause of ^{34}S-enriched sulfide) at the close of the Sturtian glaciation then we would expect that this would be followed by a gradual decline in $\delta^{34}S_{sulfate}$ as riverine sulfate input to the oceans resumes. Instead, high $\delta^{34}S_{sulfide}$ values plateau, then drop suddenly (Fig. 4). Although some postulate low sulfate concentrations in the ocean (e.g., Bottomley et al., 1992; Hurtgen et al., 2002; Strauss, 2002) the geochemical evidence presented in the previous section shows that sulfate concentration, although possibly lower than present levels, was still significant. The widespread nature of the ^{34}S-enriched post-glacial sulfides (i.e., on four continents) suggests a global event, especially since no continental reconstructions for the Neoproterozoic juxtapose these regions. Walter et al. (2000) and Gorjan et al. (2000) propose that an increase in oxygen levels in the ocean and atmosphere increased weathering of the continental sulfur ($\delta^{34}S_{sulfate} \sim +7‰$ in the modern environment) and oxidised any ^{32}S-enriched H_2S remaining in the water column, and possibly some pyrite formed during the snowball Earth period lying in the ocean depths. The evidence for this oxygenation lies in a huge swing in $\delta^{13}C_{carbonate}$ from ~0 to ~+10‰, coinciding with the drop in $\delta^{34}S_{sulfate}$, indicating a massive production and burial of organic matter with associated release of oxygen (Walter et al., 2000).

3. The $\delta^{34}S_{sulfate}$ record during the interglacial (Sturtian to Marinoan glaciations) period (Fig. 4) does not show extremely high $\delta^{34}S_{sulfate}$. $\delta^{34}S$ analyses of five anhydrite nodules from the Tapley Hill Formation show a range of +25.8 to +27.0‰. These are from a 45 m stratigraphic interval of drillhole SR-6 in South Australia, and would normally be interpreted as reflecting the true signature of seawater sulfate due to the consistency of the $\delta^{34}S_{sulfate}$ signature over a significant depth. Furthermore, only 26 m above this is a sulfate nodule in the Elatina Formation with $\delta^{34}S_{sulfate}$ of +22.3‰ (Gorjan, 1998 p. 205; Gorjan et al., 2000). However, given that there is no known way to get the mean $\delta^{34}S_{sulfide}$, which is ~+30‰ in the Tapley Hill Formation, greater than the starting $\delta^{34}S_{sulfate}$, without euxinic conditions, the nodules are tentatively interpreted as altered. Strauss (2002) also prefers a $\delta^{34}S_{sulfate}$ of +30‰ or higher, based on the elevated $\delta^{34}S_{sulfide}$ values. Hurtgen et al. (2002) report $\delta^{34}S_{sulfate}$ values between 12‰ and 51‰ in trace sulfate in the Sturtian post-glacial of the Otavi Group, northern Namibia, they interpret this large range in values as swings in the $\delta^{34}S_{sulfate}$ (Fig. 4). However, these swings do not have correlative swings in $\delta^{34}S_{sulfide}$. Furthermore, it is difficult to see values of +12‰ as producing sulfides with $\delta^{34}S_{sulfide}$ of +30‰ and above (Fig. 5).

5.7. Model

A model explaining these observations is presented in Fig. 6, based on Gorjan et al. (2000). During the Sturtian glaciation primary production in upper layers of the equatorial ocean water column drove bacterial sulfate reduction beneath a chemocline. The resultant H_2S reacted with hydrothermal iron and ^{32}S-enriched pyrite was deposited on the deep ocean floor. Residual sulfate was enriched in ^{34}S (Fig. 6(A)).

At the end of the glaciation there was a sea-level rise. The accompanying upwelling of the deep ocean brought up ^{34}S-enriched sulfate onto continental shelves (Fig. 6(B)). There was deposition of ^{34}S-enriched pyrite until massive oxygenation of the oceans and atmosphere caused weathering of continental sulfur into the oceans and oxidation of any sulfide remaining in the water column, or pyrite on the sea floor, produced during the glacial period (Fig. 6(C)). The massive oxygenation

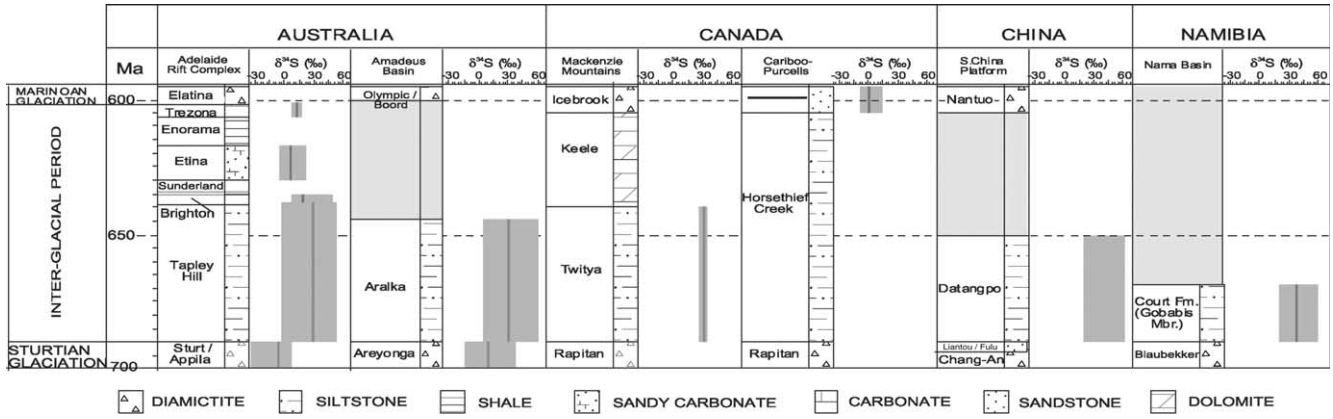

Fig. 4. $\delta^{34}S_{pyrite}$ (mean and range) from sedimentary sulfides for successions from the Sturtian to Marinoan glaciations. Adapted from Gorjan et al. (2000).

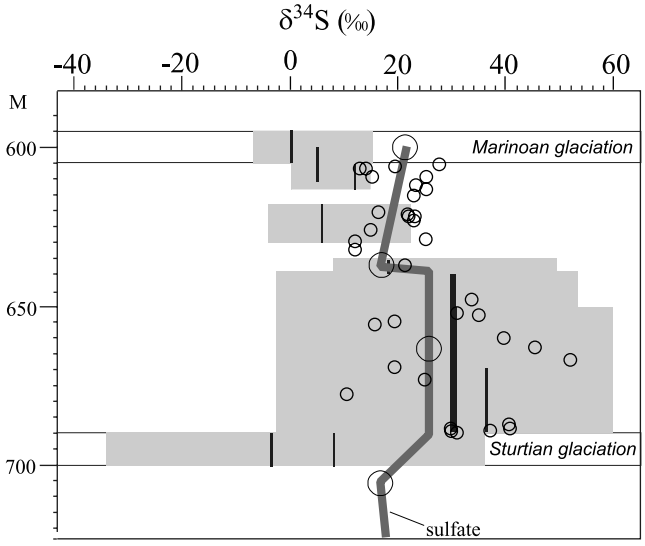

Fig. 5. $\delta^{34}S_{sulfate}$ record between the Neoproterozoic Sturtian and Marinoan glaciations. Data points from Gorjan et al. (2000) (large open circles) and Hurtgen et al. (2002) (small open circles). Shading and thin verticle lines are $\delta^{34}S_{pyrite}$ (range and mean, respectively) from Fig. 4, combined into a single column.

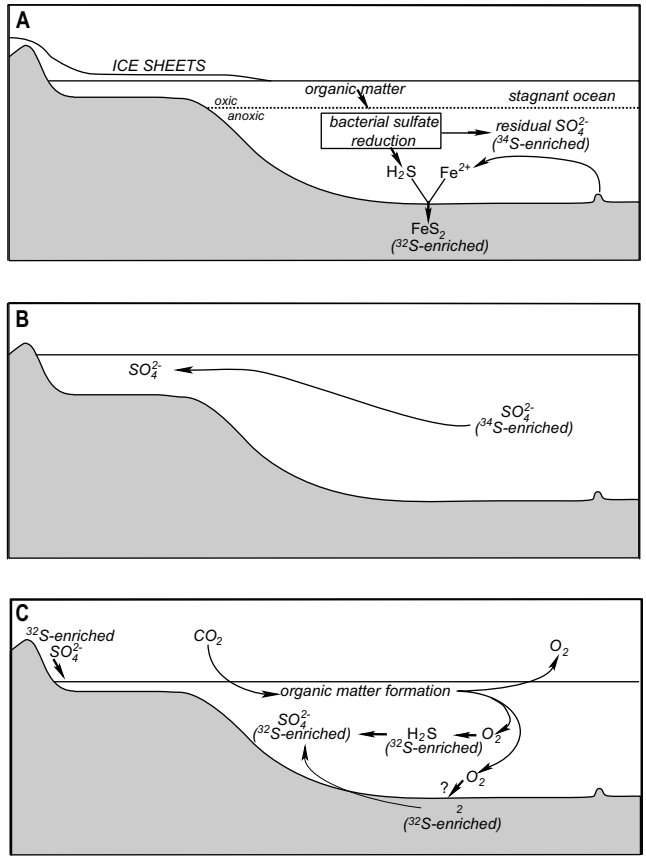

Fig. 6. Model of $\delta^{34}S_{sulfate}$ and $\delta^{34}S_{pyrite}$ rise and fall between the Neoproterozoic Sturtian and Marinoan glaciations. (A) During Sturtian glaciation. (B) Ocean-upwelling event at end of Sturtian glaciation. (C) After post-glacial silt deposition (i.e., Brighton Limestone time, from Fig. 3). Details in text. Adapted from Gorjan et al. (2000) and Gorjan (1998, p. 220).

was caused by an episode of massive burial of organic matter.

6. Conclusion

The Gobabis Member of the Court Formation, intercepted in Tahiti-1 drillhole, has extremely positive $\delta^{34}S_{pyrite}$ values, ranging from +16.1 to +61.1‰ (average = +37.6‰). $\delta^{13}C_{carbonate}$ values range from −5.2 to −2.2‰ (average = −3.7‰). On the basis of lithology, stratigraphic setting, and sulfur-isotopic composition, we correlate the Gobabis Member with Sturtian post-glacial successions in Australia, Canada, and China. Comparable units elsewhere in Namibia (Saylor et al., 1995; Hoffman et al., 1998a; Kennedy et al., 1998; Halverson et al., 1999; Yoshioka et al., 1999; Frimmel and Jiang, 2001) are likely to be the same age.

The cause of this enrichment of ^{34}S in sulfides is at present best explained by similar enrichment in $\delta^{34}S_{sulfate}$ of contemporaneous seawater (perhaps up to +60‰). This rise in seawater $\delta^{34}S_{sulfate}$ is considered to be the result of intense bacterial reduction of sulfate in an anoxic ocean during the Sturtian glaciation. The sharp drop of $\delta^{34}S_{sulfide}$ at the end of post-glacial silt deposition is explained by massive oxygenation of the oceans and atmosphere, causing weathering of continental sulfides and oxidation of ^{32}S-enriched sulfides, formed during the snowball event, to sulfate.

Acknowledgements

We acknowledge support from the Australian Research Council, Macquarie University and NAMCOR, and are grateful for the comments of John Veevers and Andrew Hill. Reviews by Galen Halverson and Wlady Altermann greatly improved the paper.

References

Alt, J.C., 1995. Sulfur isotopic profile through the oceanic crust: sulfur mobility and seawater-crustal sulfur exchange during hydrothermal alteration. Geology 23, 585–588.

Berner, R.A., 1984. Sedimentary pyrite formation: an update. Geochimica et Cosmochimica Acta 48, 605–615.

Berner, R.A., Baldwin, T., Holdren, G.R., 1979. Authigenic iron sulfides as paleosalinity indicators. Journal of Sedimentary Petrology 49, 1345–1350.

Bottomley, D.J., Veizer, J., Nielsen, H., Moczydlowska, M., 1992. Isotopic composition of disseminated sulfur in Precambrian sedimentary rocks. Geochimica et Cosmochimica Acta 56, 3311–3322.

Burton, H.R., Barker, R.J., 1980. Sulfur chemistry in an Antarctic meromictic lake. In: Freney, J., Nicholson, A.J. (Eds.), Sulfur in Australia. Australian Academy of Sciences, Canberra, pp. 96–99.

Canfield, D.E., 1998. A new model for Proterozoic ocean chemistry. Nature 396, 450–453.

Canfield, D.E., Raiswell, R., Westrich, J.T., Reaves, C.M., Berner, R.A., 1986. The use of chromium reduction in the analysis of reduced inorganic sulfur on sediments and shales. Chemical Geology 54, 149–155.

Charleson, R.J., Anderson, T.L., McDuff, R.E., 1992. The sulfur cycle. In: Butcher, S.S., Charleson, R.J., Orians, G.H., Wolfe, G.V. (Eds.), Global Biogeochemical Cycles. Academic Press, London, pp. 285–300.

Claypool, G.E., Holser, W.T., Kaplan, I.R., Sakai, H., Zak, I., 1980. The age curves of sulfur and oxygen isotopes in marine sulfate and their mutual interpretation. Chemical Geology 28, 199–260.

Condon, D.J., Prave, A.R., Benn, D.I., 2002. Neoproterozoic glacial rain-out intervals: observations and implications. Geology 30, 35–38.

Frimmel, H.E., Jiang, S.-Y., 2001. Marine evaporites from an oceanic island in the Neoproterozoic Adamastor ocean. Precambrian Research 105, 57–71.

Goldhaber, M.B., Kaplan, I.R., 1974. The sulfur cycle. In: Goldberg, E.D. (Ed.), The Sea. Wiley-Interscience, New York, pp. 569–655.

Goodfellow, W.D., Jonasson, I.R., 1984. Ocean stagnation and ventilation defined by secular trends in pyrite and barite, Selwyn Basin, Yukon. Geology 12, 583–586.

Gorjan, P., 1998. Sulfur-isotope geochemistry of the Australian Neoproterozoic. Ph.D. thesis (unpublished), Macquarie University, Australia.

Gorjan, P., Veevers, J.J., Walter, M.R., 2000. Australian Neoproterozoic sulfur-isotope geochemistry and global implications. Precambrian Research 100, 151–179.

Grotzinger, J., Knoll, A.H., 1995. Anomalous carbonate precipitates: Is the Precambrian the key to the Permian? Palaios 10, 578–596.

Halverson, G.P., Kaufman, A.J., Hoffman, P.F., Soffer, G., 1999. Stratigraphy and carbon isotopic record through the Neoproterozoic Rasthoff Formation cap carbonate, Otavi Group, Northwest Namibia. Geological Society of America—Abstracts with Programs 31 (7), 486.

Hayes, J.M., Lambert, I.R., Strauss, H., 1992. The sulfur isotopic record. In: Schopf, J.W, Klein, C. (Eds.), The Proterozoic Biosphere. Cambridge University Press, Cambridge, pp. 129–132.

Hegenberger, W., 1993. Stratigraphy and sedimentology of the late Precambrian Witvlei and Nama Groups, east of Windhoek. Geological Survey of Namibia, Memoir 17.

Hoffman, P.F., Kaufman, A.J., Halverson, G.P., 1998a. Comings and goings of global glaciation on a Neoproterozoic tropical platform. GSA Today 8, 1–9.

Hoffman, P.F., Kaufman, A.J., Halverson, G.P., Schrag, D.P., 1998b. A Neoproterozoic snowball Earth. Science 281, 1342–1346.

Hoffman, P.F., Schrag, D.P., 2002. The snowball Earth hypothesis: testing the limits of global change. Terra Nova 14, 129–155.

Hoffmann, K.H., 1989. New aspects of lithostratigraphic subdivision and correlation of late Proterozoic to early Cambrian rocks of the southern Damara Belt and their correlation with the central and northern Damara Belt and the Gariep Belt. Communications of the Geological Society of Namibia 5, 59–67.

Holser, W.T., 1992. Stable isotope geochemistry of sulfate and chloride rocks. In: Clauer, N., Chaudhuri, S. (Eds.), Isotopic Signatures and Sedimentary Rocks. Springer-Verlag, Berlin, pp. 153–176.

Hotinski, R.M., Bice, K.L., Kump, L.R., Najjar, R.G., Arthur, M.A., 2001. Ocean stagnation and end-Permian anoxia. Geology 29, 7–10.

Hurtgen, M.T., Arthur, M.A., Suits, N.S., Kaufman, A.J., 2002. The sulfur isotopic composition of Neoproterozoic seawater sulfate: implications for a snowball Earth? Earth and Planetary Science Letters 203, 413–430.

Hyde, W.T., Crowley, T.J., Baum, S.K., Peltier, W.R., 2000. Neoproterozoic 'snowball Earth' simulations with a coupled climate/ice-sheet model. Nature 405, 425–429.

Jeffries, M.O., Krouse, H.R., 1985. Isotopic and chemical investigations of two stratified lakes in the Canadian Arctic. Zietschrift fur Gletscherkunde und Glazialgeologie 21, 71–78.

Kaufman, A.J., Hayes, J.M., Knoll, A.H., Germs, G.J.B., 1991. Isotopic compositions of carbonates and organic carbon from upper Proterozoic successions in Namibia: stratigraphic variations and the effects of diagenesis and metamorphism. Precambrian Research 49, 301–327.

Kaufman, A.J., Knoll, A.H., Narbonne, G.M., 1997. Isotopes, ice-ages and terminal Proterozoic Earth history. In: Proceedings of the National Academy of Sciences USA 94, pp. 6600–6605.

Kennedy, M.J., 1996. Stratigraphy, sedimentology, and isotope geochemistry of Australian Neoproterozoic postglacial cap dolostones: degalciation, $\delta^{13}C$ excursions, and carbonate precipitation. Journal of Sedimentary Research 66, 1050–1064.

Kennedy, M.J., Runnegar, B., Prave, A.R., Hoffmann, K.H., Arthur, M.A., 1998. Two or four Neoproterozoic glaciations? Geology 26, 1059–1063.

Kennedy, M.J., Christie-Blick, N., Sohl, L.E., 2001. Are Proterozoic cap carbonates and isotopic excursions a record of gas hydrate destabilisation following Earth's coldest intervals? Geology 29, 443–446.

Lambert, I.B., Donnelly, T.H., 1988. Sedimentary sulfides: support for a Proterozoic supercontinent. Terra Cognita 8, 223.

Lambert, I.B., Donnelly, T.H., 1990. The palaeoenvironmental significance of trends in sulfur isotope compositions in the Precambrian: a critical view. In: Herbert, H.K., Ho, S.E. (Eds.), Stable Isotopes and Fluid Processes in Mineralisation. Geology Department, University of Western Australia, Special Publication 23, pp. 260–268.

Li, R., Chen, J., Zhang, S., Lei, J., Shen, Y., Chen, X., 1999. Spatial and temporal variations in carbon and sulfur isotopic compositions of Sinian sedimentary rocks in the Yangtze platform, South China. Precambrian Research 97, 59–75.

Logan, G.A., Hayes, J.M., Hieshima, G.B., Summons, R.E., 1995. Terminal Proterozoic reorganisation of biogeochemical cycles. Nature 376, 53–56.

McCrea, J.M., 1950. On the isotopic chemistry of carbonates and a paleotemperature scale. Journal of Chemical Physics 18, 849–857.

McKay, C.P., 2000. Thickness of tropical ice and photosynthesis on a snowball Earth. Geophysical Research Letters 27, 2153–2156.

Nielsen, H., 1978. Sulfur isotopes. In: Wedepohl, H. (Ed.), Handbook of Geochemistry, vol. II. Springer, Berlin, pp. 283–312.

Nriagu, J.O., Rees, C.E., Mekhtiyeva, V.L., Yu Lein, A., Fritz, P., Drimmie, R.J., Pankina, R.G., Robinson, B.W., Krouse, H.R., 1991. Hydrosphere. In: Krouse, H.R., Grinenko, V.A. (Eds.), Stable Isotopes: Natural and Anthropogenic Sulfur in the Environment. John Wiley and Sons, Chichester, pp. 177–266.

Nriagu, J.O., Coker, R.D., 1976. Emission of sulfur from Lake Ontario sediments. Limnology and Oceanography 21, 485–489.

Raiswell, R., Buckley, F., Berner, R.A., Anderson, T.F., 1988. Degree of pyritization of iron as a palaeoenvironmental indicator of bottom-water oxygenation. Journal of Sedimentary Petrology 58, 812–819.

Ross, G.M., Bloch, J.D., Krouse, H.R., 1995. Neoproterozoic strata of the southern Canadian Cordillera and the isotopic evolution of seawater sulfate. Precambrian Research 73, 71–99.

Saylor, B.Z., Grotzinger, J.P., Germs, G.J.B., 1995. Sequence stratigraphy and sedimentology of the Neoproterozoic Kuibis and Schwarzrand subgroups (Nama Basin), southwestern Namibia. Precambrian Research 73, 153–171.

Shields, G.A., Strauss, H., Howe, S.S., Siegmund, H., 2000. Sulfur-isotopic compositions from the basal Cambrian of China: implications for Neoproterozoic-Cambrian biogeochemical cycling. Journal of the Geological Society of London 156, 943–955.

Strauss, H., 1993. The sulfur isotopic record of Precambrian sulfates: new data and a critical evaluation of the existing record. Precambrian Research 63, 225–246.

Strauss, H., Banerjee, D.M., Kumar, V., 2001. The sulfur isotopic composition of Neoproterozoic to early Cambrian seawater—evidence from the cyclic Hanseran evaporites, NW India. Chamical Geology 175, 17–28.

Strauss, H., 2002. The isotopic compostion of Precambrian sulphides—seawater chemistry and biological evolution. In: Altermann, W., Corcoran, P.L. (Eds.), Precambrian Sedimentary Environments: A Modern Approach to Ancient Depositional Systems. Special publication 33 of the International Association of Sedimentologists. Blackwell Science, Malden, MA, pp. 67–105.

Thode, H.G., 1991. Sulfur isotopes in nature and the environment: an overview. In: Krouse, H.R., Grinenko, V.A. (Eds.), Stable Isotopes: Natural and Anthropogenic Sulfur in the Environment. Wiley, Chichester, pp. 1–26.

Tuttle, M.L., Goldhaber, M.B., 1993. Sedimentary sulfur geochemistry of the Palaeogene Green River Formation, western USA: Implications for interpreting depositional and diagenetic processes in saline alkaline lakes. Geochimica et Cosmochimica Acta 57, 3023–3039.

Walter, M.R., Veevers, J.J., Calver, C.R., Gorjan, P., Hill, A.C., 2000. Dating the 830-544 Ma late Neoproterozoic interval by isotopes of strontium, carbon (carbonate and organic), and sulfur (sulfate) in seawater. Precambrian Research 100, 371–433.

Xu, X., Huang, H., Liu, B., 1990. Manganese deposits of the Proterozoic Datangpo formation, South China: genesis and palaeogeography. In: Sediment-Hosted Mineral Deposits. Special publication of the International Association of Sedimentologists 11, pp. 39–50.

Yoshioka, H., Tojo, B., Kawakami, S., Okaniwa, T., Takano, M., Hoffman, P.F., 1999. Secular variations of carbon and oxygen isotopic compositions of the Neoproterozoic Rasthoff cap carbonates in Namibia. Geological Society of America—Abstracts with Programs 31 (7), 486.